

УДК 539.12

STRUCTURE OF BACKGROUND IN HEIDELBERG–MOSCOW EXPERIMENT ON SEARCH FOR AND INVESTIGATION OF DOUBLE BETA DECAY OF ^{76}Ge

K. Ya. Gromov, V. A. Bednyakov¹, V. I. Fominykh, V. G. Chumin

Joint Institute for Nuclear Research, Dubna

Independent analysis of the spectra from the Heidelberg–Moscow experiment has been carried out. A direct comparison of the peak intensities in the spectra allows a conclusion that in the energy range up to 3200 keV the background is due to detection of γ rays from the decay of trace impurities of anthropogenic and cosmogenic nuclides occurring in the apparatus between the HPGe detectors and the main (Pb and Cu) shielding. The ^{226}Ra , ^{214}Pb , and ^{214}Bi γ rays observed in the spectra are shown to arise in the ^{226}Ra rather than ^{238}U decay chain. The estimates of the expected intensities of weak ^{214}Bi γ rays in the spectrum region in the vicinity of $Q_{\beta\beta}(^{76}\text{Ge}) = 2039$ keV do not contradict observation of the peak at 2039 keV as claimed by Klapdor-Kleingrothaus and coauthors.

Выполнен независимый анализ спектров эксперимента Гейдельберг–Москва. Результаты непосредственного сравнения интенсивностей пиков в спектрах позволяют заключить, что фон в области энергий до 3200 кэВ возникает при регистрации γ -лучей от распада малых, следовых примесей антропогенных и космогенных нуклидов, расположенных в установке между HPGe-детекторами и основной (Pb и Cu) защитой. Показано, что наблюдаемые в спектрах γ -лучи ^{226}Ra , ^{214}Pb и ^{214}Bi возникают в цепочке распадов ^{226}Ra , а не ^{238}U . Оценки ожидаемых интенсивностей слабых γ -лучей ^{214}Bi на участке спектра в окрестности $Q_{\beta\beta}(^{76}\text{Ge}) = 2039$ кэВ не противоречат тому, что пик 2039 кэВ, открытие которого объявлено Клапдор-Клайнгротхаузом и соавторами, действительно не наблюдается.

INTRODUCTION

The double neutrinoless beta decay ($0\nu 2\beta$ decay) of nuclei

$$A(Z, N) \rightarrow A(Z + 2, N - 2) + 2e^{-},$$

which may proceed only with violation of the lepton number conservation law by two units ($\Delta L = 2$), is generally recognized to be a process of high scientific significance. Experimental observation of the $0\nu 2\beta$ decay is of great interest as direct and unambiguous indication of going beyond the standard model of electroweak interactions where the lepton number is strictly conserved ($\Delta L = 0$). In addition, by the Schechter–Valle theorem [1] the probability of the $0\nu 2\beta$ decay means that at least one of the neutrinos has a nonzero mass and, moreover,

¹E-mail: Vadim.Bednyakov@jinr.ru

that the neutrino is a Majorana particle (i.e., has a Majorana nature, when the particle coincides with its antiparticle).

Many collaborations in various underground laboratories have been trying to detect the neutrinoless beta decay using various isotopes potentially capable of decaying via the $0\nu 2\beta$ mode, such as Ge, Se, Mo, Cd, Te, Xe. The currently best result has been obtained in the joint German–Russian Heidelberg–Moscow experiment with five large highly pure Ge detectors enriched with germanium-76, which are located deep underground in the Gran Sasso low-background laboratory (Italy). The limit for the $0\nu 2\beta$ -decay period of ^{76}Ge was established to be $T_{1/2}(0\nu 2\beta) \geq 1.9 \cdot 10^{25}$ y (90% C.L.) [2]. Later the spectral region expected to embrace the energy of the ^{76}Ge double beta decay ($Q_{\beta\beta} = 2039.0$ keV) was thoroughly analyzed again under the supervision of Prof. Klapdor-Kleingrothaus, and the results of the analysis allowed the authors to state observation of a peak at 2039 keV in the spectrum [3–5]. In the same spectral region lines of energy 2011, 2017, 2022 and 2053 keV were detected and ascribed to the ^{214}Bi decay [6].

Soon after Klapdor-Kleingrothaus and coauthors reported observation of the 2039-keV peak [3, 4] there appeared papers by C. E. Aalseth et al. [7], F. Feruglio et al. [8], and Yu. G. Zdesenko et al. [9], questioning observation of the ^{76}Ge $0\nu 2\beta$ decay in [3, 4]. It is stated in [7] and [9] that the ^{214}Bi γ lines and the 2039-keV line observed by Klapdor-Kleingrothaus et al. [3, 4] are spurious. In [8] this spectral region was analyzed by the same methods as in [3, 4] and practically the same lines as in [3, 4] were revealed. It was stressed, however, that more accurate data on the background structure in this spectral region were needed to draw a final conclusion. The well-grounded answer to this criticism was first given by Klapdor-Kleingrothaus in [10] and then the observation of this line was supported by the results of special additional investigations published by the authors within the year [11–18]. The results of the most complete analysis of the background spectrum of the Heidelberg–Moscow experiment obtained with careful Monte-Carlo simulation based on the GEANT4 package are published in [19].

Yet, it was of interest to find out what conclusions about the background structure could be drawn from a direct comparison of the peak intensities observed in the background spectrum. To do this, Prof. Klapdor-Kleingrothaus kindly provided the authors of this paper with the files of three spectra measured in the Heidelberg–Moscow experiment. Spectrum I is a total spectrum of all 5 detectors (Nos. 1, 2, 3, 4, and 5) measured over the period from August 1990 to May 2000 in the energy range up to 2850 keV (it corresponds to Fig. 3 from [5]). Spectrum II is the total spectrum of all 5 detectors (Nos. 1, 2, 3, 4, and 5) measured over the period from August 1995 to May 2000 in the energy range up to 8350 keV. Spectrum III is the spectrum of detector No. 4 measured over the period from August 1995 to May 2000 in the energy range up to 8350 keV.

The Heidelberg–Moscow experimental setup is described in detail, for example, in [5, 20]. It should be noted that Spectrum III is of particular interest because detector No. 4 has additional Cu shielding 27.5 cm thick installed between this detector and the lead shielding.

1. IDENTIFICATION OF γ LINES IN THE BACKGROUND SPECTRUM

The results yielded by our analysis of Spectrum I (Fig. 3 from [5]), including γ -ray energies, intensities (areas of photopeaks), and identifications are presented in Table 1. To

identify γ rays we used Firestone's Tables of Isotopes (hereinafter referred to as TI) [6], tables of the Japanese Institute of Atomic Energy (JAERI-Data, Code 98-008 and JNDC(JPN)-170/L), and tables «Gamma-ray from radioactive decay, listed in order of increasing energy» by U. Rous, W. Westmeier, I. Warneke (Magdeburg; Darmstadt, 1978).

The following possible cases were considered:

— γ rays arise from the decay of nuclides belonging to the radioactive ^{238}U ($4n + 2$) or ^{232}Th ($4n$) families;

— γ rays arise from the decay of long-lived anthropogenic nuclides;

— γ rays arise from the decay of cosmogenic (n, γ or μ^-, γ) nuclides.

Column 3 of Table 1 shows nucleus (A, Z) to which the particular decay γ transition is ascribed. Columns 4 and 5 show the energy of this γ transition and the intensity, a_γ , of the γ rays per decay of the nucleus (per decay in the radioactive chain) from the TI [6]. The last column presents the calculated ratios $\frac{S_{\gamma i}}{a_{\gamma i}} = N\varepsilon(E_{\gamma i})$ (see formula (2) below). We skip figures with used experimental spectra, because they are qualitatively the same as in [2, 19]. Our conclusions given below rely on quantitative analysis of the intensities of the lines in these spectra.

($4n + 2$) **Chain Decay Nuclei.** Energies of 25 γ lines allow them to be ascribed to the decay of the ^{214}Pb ($T_{1/2} = 26.8$ min) and ^{214}Bi (19.7 min) nuclei from this chain. They are short-lived nuclei arising from the decay of a long-lived parent nucleus in the setup. Radiations of short-lived nuclides from the ($4n + 2$) family observed in the background spectra are usually attributed to uranium contamination of the setup, the short-lived nuclides assumed to be in secular equilibrium with uranium. Yet, one overlooks the fact that in the uranium-238 family the short-lived nuclei ^{226}Ra ($1.6 \cdot 10^3$ y), ^{214}Pb (26.8 min) and ^{214}Bi (19.7 min) are preceded by the long-lived nuclei ^{234}U ($2.5 \cdot 10^5$ y) and ^{230}Th ($7.5 \cdot 10^4$ y). Therefore, accumulation of ^{226}Ra and daughter nuclei in the time after separation of impurity uranium from the ore should be ignored and the ^{226}Ra , ^{214}Pb and ^{214}Bi γ lines in the spectra should be ascribed to radium-226 contamination of the setup. The presence of ^{238}U in the Heidelberg–Moscow setup could be estimated from the spectral γ lines of ^{234m}Pa (1.17 min) which is in equilibrium with ^{238}U . The observed 1001.9 keV γ decay can be ascribed to the ^{234m}Pa decay and identified as the highest-intensity transition in this decay. However, the intensity of this spectral line is very low ($S_\gamma \cong 0.09 \cdot 10^3$). No other evidence for the presence of ^{238}U in the setup was found. Thus, contamination of the setup by ^{238}U is not proved.

The number of detected decays of a nucleus followed by emission of γ rays with energy E_γ (i.e., the photopeak area $S(E_\gamma)$) is given by the expression

$$S(E_\gamma) = Na(E_\gamma)\varepsilon(E_\gamma), \quad (1)$$

where N is number of decays of the nucleus within the time of the experiment; $a(E_\gamma)$ is the intensity of the γ rays with energy E_γ per decay of the nucleus (per decay in the equilibrium chain); $\varepsilon(E_\gamma)$ is the detection efficiency for γ rays with the energy E_γ at the photopeak. Column 6 of Table 1 presents the calculated quantities

$$N\varepsilon(E_{\gamma i}) = \frac{S_{\gamma i}}{a_{\gamma i}}. \quad (2)$$

We have no data which allows us to determine N and $\varepsilon(E_\gamma)$ separately, but even their product allows some helpful conclusions. Dependence of $N\varepsilon(E_\gamma)$ on E_γ for the ^{226}Ra , ^{214}Pb and

Table 1. Spectrum I analysis results. Gamma rays of energies 230 to 2850 keV in the Heidelberg–Moscow experiment

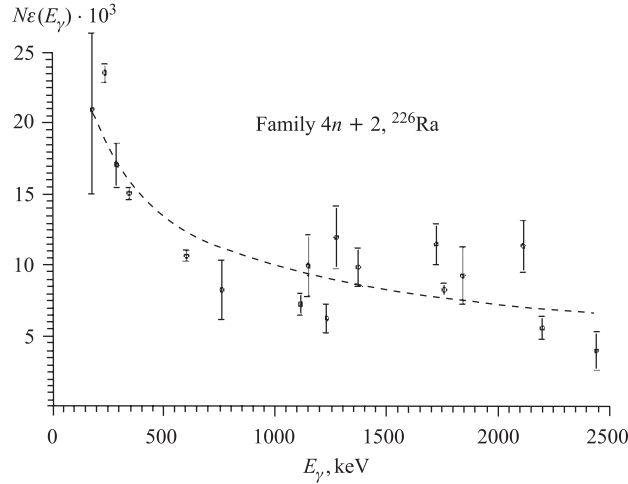
Experiment		Identification			$N\varepsilon(E_\gamma) \cdot 10^{-3}$
E_γ , keV	$S_\gamma \cdot 10^{-3}$	A_Z	E_γ , keV	a_γ	
186.0(2)	0.7(2)	${}^{226}\text{Ra}$	186.21	0.033	21(6)
238.68(10)	5.51(15)	${}^{212}\text{Pb}$	238.63	0.433	12.7(4)
241.83(14)	1.77(5)	${}^{214}\text{Pb}$	241.98	0.075	23.6(7)
295.22(10)	3.16(22)	${}^{214}\text{Pb}$	295.21	0.115	17.1(18)
299.7(3)	0.39(3)	${}^{212}\text{Pb}$	300.09	0.033	11.9(9)
328.30(10)	~ 0.3	${}^{228}\text{Ac}$	328.0	0.030	~ 10.2
337.8(2)	0.83(16)	${}^{228}\text{Ac}$	338.3	~ 0.113	~ 7.4
339.5(3)	0.37(14)	${}^{228}\text{Ac}$	341.0	0.0038	97
347.5(4)	0.16(10)	${}^{214}\text{Bi}$	348.0	0.0068	200
351.90(10)	5.40(15)	${}^{214}\text{Pb}$	351.92	0.358	15.1(4)
409.7	$\sim 0.17(14)$	${}^{228}\text{Ac}$	409.45	0.019	~ 8.9
427.86(14)	0.68(11)	${}^{125}\text{Sb}$	427.88	0.30	2.3(4)
463.05(17)	0.53(14)	${}^{228}\text{Ac}$	463.0	0.044	12(3)
		${}^{125}\text{Sb}$	463.4	0.105	5.0(3)
511.11(13)	1.70(19)	${}^{208}\text{Tl}$	510.77	0.082	21(2)
569.77(14)	0.59(6)	${}^{207}\text{Bi}$	569.70	0.977	0.60(9)
579.90(10)	0.193(10)				
583.20(11)	1.72(9)	${}^{208}\text{Tl}$	583.19	0.307	5.6(3)
600.50(14)	0.58(7)	${}^{125}\text{Sb}$	600.60	0.175	3.3(4)
609.27(10)	4.8(2)	${}^{214}\text{Bi}$	609.31	0.448	10.7(4)
622.80(10)	0.15(3)				
635.9(3)	0.36(7)	${}^{125}\text{Sb}$	635.95	0.112	3.2(6)
661.66(10)	14.3(3)	${}^{137}\text{Cs}$	661.66	0.851	16.8(3)
727.3(2)	0.31(10)	${}^{212}\text{Bi}$	727.33	0.066	4.7(15)
768.11(10)	0.40(10)	${}^{214}\text{Bi}$	768.36	0.048	8.3(21)
785.6(3)	0.15(5)	${}^{212}\text{Bi}$	785.37	0.011	13.6(45)
795.45(16)	0.40(6)	${}^{228}\text{Ac}$	795.00	0.0434	9.2(14)
~ 802	~ 0.3				
~ 806	~ 0.24	${}^{214}\text{Bi}$	806.17	0.0112	~ 21
~ 810	~ 0.13	${}^{58}\text{Co}$			
834.9(2)	0.46(11)	${}^{54}\text{Mn}$			
840.6(2)	0.33(10)	${}^{228}\text{Ac}$	840.4	0.0093	35(10)
860.66(10)	0.24(8)	${}^{208}\text{Tl}$	860.56	0.045	5.3(18)
910.93(11)	1.78(12)	${}^{228}\text{Ac}$	911.2	0.266	6.5(15)
934.01(10)	~ 0.37	${}^{214}\text{Bi}$	934.04	0.0303	~ 12
964.82(10)	0.26(2)	${}^{228}\text{Ac}$	964.77	0.051	5.1(4)
968.65(12)	0.78(6)	${}^{228}\text{Ac}$	968.97	0.162	4.8(4)
999.7(3)	0.09(5)				
~ 1001.9	$\sim 0.05(2)$	${}^{234}\text{Pa}$	1001.0	0.0084	~ 6.0
1063.70(10)	0.44(7)	${}^{207}\text{Bi}$	1063.66	0.745	0.59(9)
1093.5	0.10(5)	${}^{228}\text{Ac}$	1095.68	0.0013	77(38)
1120.16(14)	1.08(11)	${}^{214}\text{Bi}$	1120.29	0.148	7.3(7)
1124.3(3)	0.38(7)				

Table 1 (continued)

Experiment		Identification			$N\varepsilon(E_\gamma) \cdot 10^{-3}$
E_γ , keV	$S_\gamma \cdot 10^{-3}$	A_Z	E_γ , keV	a_γ	
1147.3	0.11(5)				
1155.4(3)	0.17(6)	${}^{214}\text{Bi}$	1155.19	0.0164	10.4(36)
1173.21(11)	3.42(14)	${}^{60}\text{Co}$	1173.2	1.00	3.42(14)
1237.82(10)	0.37(6)*	${}^{214}\text{Bi}$	1238.11	0.0586	6.3(10)
1281.6(1)	0.17(4)	${}^{214}\text{Bi}$	1280.96	0.0144	11.8(28)
1332.46(12)	3.21(13)	${}^{60}\text{Co}$	1332.47	1.00	3.21(13)
1363.4(5)	0.08(2)				
1377.5(2)	0.39(5)	${}^{214}\text{Bi}$	1377.67	0.392	9.9(13)
1401.10(10)	~ 0.11	${}^{214}\text{Bi}$	1401.50	0.0155	~ 7.1
1407.6(3)	0.22(5)	${}^{214}\text{Bi}$	1408.0	0.028	~ 7.8
1460.48(12)	9.50(19)	${}^{40}\text{K}$	1460.81	0.105	90.5(20)
~ 1509	~ 0.08	${}^{214}\text{Bi}$	1509.23	0.021	~ 4
~ 1587	~ 0.05	${}^{228}\text{Ac}$	1588.21	0.0327	~ 1.5
1620.4(2)	0.08(2)	${}^{212}\text{Bi}$	1620.5	0.015	5.3(13)
~ 1630	~ 0.04	${}^{228}\text{Ac}$	1630.6	0.016	~ 2.5
~ 1660	~ 0.10	${}^{214}\text{Bi}$	1661.3	0.0114	~ 9
1729.3(2)	0.33(4)	${}^{214}\text{Bi}$	1729.60	0.0288	11.5(14)
1764.4(2)	1.27(6)	${}^{214}\text{Bi}$	1764.49	0.154	8.3(4)
1847.5(2)	0.19(4)	${}^{214}\text{Bi}$	1847.42	0.0204	9.3(20)
2102.8(9)	0.07(3)	${}^{208}\text{Tl}$	SEP 2614.5		
2118.3(3)	0.13(2)	${}^{214}\text{Bi}$	2118.55	0.0114	11.4(18)
2204.2(2)	0.27(4)	${}^{214}\text{Bi}$	2204.21	0.0486	5.6(8)
2292.1(3)	0.034(17)	(${}^{214}\text{Bi}$)	2293.4	0.0030	11(6)
2447.8(2)	0.06(2)	${}^{214}\text{Bi}$	2447.86	0.015	4.0(13)
2505.9(2)	0.10(2)	${}^{60}\text{Co}$	$\Sigma 1172 + 1332$		
2614.5(1)	0.82(5)	${}^{208}\text{Tl}$	2614.5	0.36	2.28(14)

${}^{214}\text{Bi}$ γ lines is displayed in figure. Though the errors in the values $N\varepsilon(E_\gamma)$ are large, these values may be assumed to increase monotonically as the energy decreases, which additionally confirms that the nuclei in question belong to one equilibrium chain, namely, the ${}^{226}\text{Ra}$ chain. The $N\varepsilon(E_\gamma)$ value for the 347.5-keV γ transition which drops out of the smooth dependence probably indicates the presence of another, unidentified background nuclide emitting γ rays of the same energy. In the equilibrium chain N is constant. Therefore, an increase in the region of low energies ($E_\gamma < 500$ keV) directly indicates that a considerable number of all ${}^{226}\text{Ra}$, ${}^{214}\text{Pb}$ and ${}^{214}\text{Bi}$ nuclei decay in the close vicinity to the detectors (between the detectors and the passive shielding).

4n Decay Chain Nuclei. The γ -ray energies (Table 1) allow about 20 γ transitions to be ascribed to the decay of the nuclei from this chain: ${}^{228}\text{Ac}$ ($T_{1/2} = 6.1$ h), ${}^{212}\text{Pb}$ (10.6 h), ${}^{212}\text{Bi}$ (60.6 min) and ${}^{208}\text{Tl}$ (3.1 min). Monotonic dependence of $N\varepsilon(E_\gamma)$ on the γ -ray energy does not contradict (see Table 1) the fact that the above nuclides are produced in one equilibrium decay chain. The parent long-lived nucleus of this chain may be ${}^{232}\text{Th}$ ($1.4 \cdot 10^{10}$ y) or ${}^{228}\text{Ra}$ (5.8 y). An increase in $N\varepsilon(E_\gamma)$ in the region $E_\gamma < 500$ keV indicates that long-lived parent nuclei whose decay results in the above nuclei are localized in the vicinity of the detectors (between the passive shielding and the detectors). Spectrum II and Spectrum III show a


 Dependence of $N\varepsilon(E_\gamma)$ on E_γ for γ lines from the ^{226}Ra chain decay

peak at 3199 keV which we identify as a peak of a sum of pulses from the γ -ray cascade $584.2 + 2614.5 = 3198.7$ keV. Formation of the sum peak also indicates that ^{208}Tl decays in close vicinity to the detectors.

^{60}Co Beta Decay. The transitions γ_{1173} ($N\varepsilon(E_\gamma) = 3420$) and γ_{1332} ($N\varepsilon(E_\gamma) = 3210$) are ascribed to this decay. All three spectra show a 2505-keV peak of the sum of pulses from these transitions. The estimated average γ_{1173} and γ_{1332} detection efficiency about 3% indicates that ^{60}Co nuclei decay in close vicinity to the detectors.

Gamma Rays from the ^{125}Sb Decay. Four γ transitions (Table 1) can be ascribed on the basis of E_γ to the β^- decay of ^{125}Sb . The energy of one of them, 463.4 keV, coincides with 463.0 from the ^{228}Ac decay within the error. Taking $N\varepsilon(E_\gamma)$ for the ^{228}Ac 463.0-keV γ line to be approximately $7 \cdot 10^3$, as for the neighboring γ rays from the $4n$ chain, we get $N\varepsilon(E_\gamma) \sim 3 \cdot 10^3$ for the ^{125}Sb γ line at 463.4 keV. Table 2 lists energies of the γ rays ascribed to the ^{125}Sb decay and $N\varepsilon(E_\gamma)$ for them. Thus, $N\varepsilon(E_\gamma)$ values can be considered as being not in conflict with ascribing the above γ lines to the decay of the same ^{125}Sb nucleus.

 Table 2. ^{125}Sb γ rays observed in Spectrum I

E_γ, keV	427.9	463.4	600.5	635.9
$N\varepsilon(E_\gamma)$	$2.3(4) \cdot 10^3$	$\sim 3 \cdot 10^3$	$3.3(4) \cdot 10^3$	$3.2(6) \cdot 10^3$

Gamma Rays from the Electron Capture Decay of Nuclei. There is no doubt about identification of γ rays at 1460.8 keV ($\beta^+\text{EC } ^{40}\text{K}$, $N\varepsilon(E_\gamma) = 90500$), 569.7 and 1063.7 keV (EC ^{207}Bi , $N\varepsilon(E_\gamma) = 600$ and 590). Dörr and Klapdor-Kleingrothaus [19] ascribe four more peaks to the nuclei undergoing electron capture decay. They assumed that the $E_\gamma \approx 810$ keV peak results from electron capture in the ^{58}Co ($T_{1/2} = 70.8$ d) nucleus, the $E_\gamma = 834.9$ keV arises from the EC in the ^{54}Mn ($T_{1/2} = 312$ d) nucleus, the $E_\gamma = 840.6$ keV peak is due to summation of pulses from $E_\gamma = 834.9$ keV and x rays, and the $\gamma_{1124.3}$ peak is caused by summation of 1115.2-keV γ rays and x rays arising from electron capture in the ^{65}Zn

($T_{1/2} = 244$ d) nucleus. The ^{58}Co , ^{54}Mn , and ^{65}Zn nuclei are relatively short-lived ones, and their radiation may manifest itself in the spectrum as their residual activity after being left to stand for 200 days before the beginning of data collection [5]. In the course of the experiment the intensity of the above γ lines should considerably (in approximately 10 years) decrease. Under this condition identification of $E_\gamma \approx 810$ keV, $E_\gamma = 834.9$ keV, and $E_\gamma = 840.6$ keV does not contradict anything.

In Table 1 the 840.6-keV line is ascribed to the ^{228}Ac decay while the value $N\varepsilon(E_\gamma) = 35(10) \cdot 10^3$ is a few times larger than that of the neighboring ^{228}Ac lines. With the contribution to the 840.6-keV peak from the sum of $E_\gamma = 834.9$ keV and x rays taken into account, $N\varepsilon(E_\gamma)$ approaches the average value at this energy for the $4n$ chain. Interpretation of the 1124.3-keV line as a sum of pulses from $E_\gamma = 1115.2$ keV and x rays following EC in ^{65}Zn is a different matter. The fluorescence yield in this Z region is $\omega_k = 0.47$. If ^{65}Zn nuclei as the other setup impurities are located outside the detectors, then the x-ray detection efficiency (solid angle «source-detector») should be < 1 and a peak at $E_\gamma = 1115.2$ keV should appear in the spectrum with intensity larger than the intensity of the peak of the sum with the x rays. The peak $E_\gamma = 1115.2$ keV can completely disappear due to summing with x rays and Auger electrons only in the case when ^{65}Zn is located inside the material of the detectors. This is scarcely probable. Therefore, we believe the 1124.3-keV line has to be explained.

The analysis of Spectrum II and Spectrum III in the region up to 2850 keV yields results that generally agree within the errors with the results yielded by the analysis of Spectrum I (Table 1). Spectrum III measured with a copper shield (27.5 cm) between the main lead shielding and the detector allows the conclusion that the background from external sources (rocks in the underground laboratory) is negligibly small, i.e., that it is small impurities between the main shielding and the detectors which are responsible for the background in the Heidelberg–Moscow experiment. An appreciable (5–7 times) decrease in the intensity of the γ 661-keV peak from the ^{137}Cs decay in Spectrum III may indicate that the ^{137}Cs nuclide is present in the lead shielding, though contamination of the assembly of detectors Nos. 1, 2, 3, 5 with ^{137}Cs is not impossible either. Finally, a comparison of Spectra I and II with Spectrum III is in conflict with the assertion (Table 2 in [19]) that the ^{40}K and ^{210}Pb nuclides are present in the lead shielding materials.

It is difficult to analyze Spectra II and III in the region above 3500 keV because there are no reference energy values in this region. A wide peak at about 5240 keV manifests itself in both spectra. In [5, 20] and [21] this peak is said to be due to detection of α particles from the decay of ^{210}Po ($T_{1/2} = 138$ d, $E_{\alpha 0} = 5305$ keV, $I_{\alpha 0} = 100\%$), produced in the β^- decay of ^{210}Pb ($T_{1/2} = 22.3$ y). It is assumed that ^{210}Pb is located on the inner surface of the detector shell. The energy of the α particles decreases (by ~ 70 keV) as they pass through the dead surface layer of the detectors.

Bakalyarov et al. [21] simulated the background spectrum of all the five detectors in the region of 3500–8000 keV. They believe that the observed spectrum is satisfactorily explained by detection of α particles from the decay of nuclides of the uranium and thorium equilibrium chains on the assumption that uranium and thorium nuclei are located, like ^{210}Pb nuclei, on the inner surface of the shell of the detectors. However, this conclusion does not agree with the above assertion that observation of ^{226}Ra , ^{214}Pb , and ^{214}Bi in the background spectrum is caused by contamination of the setup with ^{226}Ra rather than ^{238}U . If the setup is contaminated with a small amount of uranium, this may cause observation of radiation from ^{238}U ($4.5 \cdot 10^9$ y), ^{234}Th (24.1 d), ^{234m}Pa (1.2 min), and ^{234}U ($2.5 \cdot 10^5$ y) in the background

spectrum. The peaks due to α particles from the decay of ^{230}Th ($8 \cdot 10^4$ y, $E_{\alpha 0} = 4.77$ MeV, $I_{\alpha 0} = 76\%$) are ruled out in the spectrum. Therefore, we think that explanation of the events observed in the energy region above 3500 keV needs more careful consideration.

The Results of Identification of γ Rays in the background spectrum of the Heidelberg–Moscow experiment are summarized in Table 3.

Table 3. Results of identification of γ rays in the background spectrum

A_Z	$T_{1/2}$, y	E_γ , keV	$N\varepsilon(E_\gamma)$	Q_{β^-} or Q_{EC} , keV
$^{226}\text{Ra} \rightarrow$	$1.6 \cdot 10^3$	25- γ	2400–5000	^{214}Bi , β^- 3270 ^{210}Tl , β^- 5497
$^{232}\text{Th} \rightarrow$	$1.4 \cdot 10^{10}$	21- γ	1300–2300	^{208}Tl , β^- 4992
^{40}K	$1.3 \cdot 10^9$	1460	90500	EC 1505
^{60}Co	5.3	1172; 1332	3300	β^- 2824
^{137}Cs	30.2	661.7	16800	EC 1220
^{125}Sb	2.7	422.9; 463.0; 600.6; 635.9	3000	β^- 767
^{207}Bi	38	569.7; 1063.7	600	EC 2405
^{54}Mn	0.85	834.9 (840.6)	460	EC 1377
^{58}Co	0.19	810	130	EC 2307

The table presents A , Z , $T_{1/2}$ of the isotope whose γ rays are observed in the background spectrum, and energies of the γ rays (for the ^{226}Ra and ^{238}Th equilibrium chains there are the numbers of γ transitions identified in the chain). Column 4 lists values $N\varepsilon(E_\gamma) = \frac{S(E_\gamma)}{a(E_\gamma)}$ (see formula (2)) which allow an idea about the number of detected decays. It should be borne in mind, of course, that the detection efficiency decreases with increasing E_γ and depends on the place where these nuclei decay. The last column of Table 3 lists energies of the β^- decay (Q_{β^-}) or EC (Q_{EC}) of the corresponding isotopes. For the ^{226}Ra and ^{232}Th decay chains there are energies of the β decay of the chain member isotopes for which $Q > 2000$ keV and whose decay may give rise to 2039-keV γ rays of interest. For the five nuclides Q_{β^-} or Q_{EC} is larger than 2000 keV. But comparison of the available TI data [6] on their γ spectra with the intensities of the spectral γ lines given in Table 1 allows the presence of the 2039-keV line to be ruled out.

However, it is not impossible that some γ transitions from Table 1 proceed in reactions with background neutrons and μ mesons. These reactions could be followed not only by γ rays from the decay of the corresponding nuclide but also by high-energy γ rays. In this connection it is of interest to trace the variation in the intensity of γ rays over the exposure period (13 years) of the Heidelberg–Moscow experiment. It might be possible to observe the expected decrease in the intensity of ^{125}Sb and ^{60}Co γ rays as well as disappearance of the γ rays ascribed to the ^{54}Mn and ^{58}Co decay. A decrease in the intensity of the γ rays from the decay of the nuclides belonging to the $4n$ chain may indicate that this chain begins with ^{228}Ra ($T_{1/2} = 5.8$ y) nucleus. An increase in the intensity of some lines may also be observed.

2. SPECTRAL REGION OF 2000–2060 keV

C. E. Aalseth et al. [7] and Yu. G. Zdesenko et al. [9] state that weak γ lines of ^{214}Bi , observed by Klapdor-Kleingrothaus et al. [3–5] in the spectral region 2000–2060 keV *cannot manifest themselves* in the spectrum. Accordingly, the 2039.0-keV line with the intensity close to the intensity of those weak Bi lines could not be observed either.

Table 4. Experimental and calculated (expected) intensities of weak peaks from the ^{214}Bi decay. Row 1: experimental intensities of peaks according to [10]; row 2: intensities of γ rays per ^{214}Bi decay; row 3: expected intensities of peaks (summation of pulses is ignored); row 4: the same as in row 3 but according to [7]; row 5: intensities of peaks calculated in [10] with summation of peaks taken into account

No.	E , keV	$\gamma_{2204.2}$	$\gamma_{2010.7}$	$\gamma_{2016.7}$	$\gamma_{2021.8}$	$\gamma_{2052.9}$	$\gamma_{2039.0}$
1	S_{exp} from [10]	319(22)	37.8(102)	13.0(85)	16.7(88)	23.2(90)	12.1(83)
2	$a_{\gamma}\%$ according to [6]	4.86	0.050(6)	$\equiv 0$	0.020(6)	0.078(11)	
3	$S = 319 \cdot a_{\gamma i} / 4.86$	319	3.3(4)	$\equiv 0$	1.3(4)	5.1(7)	
4	S according to [7]	319	3.2	0.38	1.26	5.0	
5	$S_{\gamma i} + S_{\Sigma}$ from [10]	319	12.2(6)	15.6(7)	1.2(1)	4.7(3)	

In Klapdor-Kleingrothaus's reply [10] to the criticism [7], and in [5] intensities of peaks in the region 2000–2060 keV are evaluated. They are presented in the first row of Table 4. Expected intensities of weak ^{214}Bi peaks can be found by using intensities of strong ^{214}Bi lines in the background spectrum and data on intensities of ^{214}Bi decay γ rays from the TI [6] (row 2 in Table 4). The detection efficiency for γ rays in the region 2000–2060 keV and the detection efficiency for 2204-keV γ rays can be considered identical within errors, and the expected intensities of weak ^{214}Bi γ rays can be calculated by using intensities of 2204-keV γ rays in the background spectrum. The results of these calculations are presented in row 3 of Table 4. Row 4 presents the results of similar evaluations from [7] normalized to the intensity of the 2204-keV γ peak equal to 319 events in [10] (row 1 of the table). The values in rows 3 and 4 are seen to coincide except the value for the 2016.7-keV peak. The values for $S_{\gamma_{2016.7}}$ in [7] is calculated incorrectly. According to the TI [6], the intensity of 2016.7-keV γ rays is identically equal to zero because it is a transition of the $E0$ type. In [7], for the intensity of 2016.7-keV γ rays they used the intensity of conversion electrons of this γ transition [6]. The experimentally observed peak at 2016.7 keV should be attributed to summation of pulses from cascade γ transitions of 1408 and 609 keV from the 0^+ 2016.7-keV level to the 0^+ ground state of ^{214}Po in the decay of ^{214}Bi . According to the ^{214}Bi decay scheme, a considerable pulse summation effect should also be responsible for formation of the 2010.7-keV peak (as a cascade $1401 + 609 = 2010$ keV). Thus, reliability of observation of weak ^{214}Bi lines can be estimated only from the peaks at 2021.8 and 2052.9 keV, whose intensity, according to the ^{214}Bi decay scheme, suffers only an insignificant (below 1%) decrease due to summation in the spectrum.

Analyzing Spectrum I, we obtained the intensity of the γ 2204-keV peak equal to 290(30) events, which agrees with the 319(22) events found in [5, 10]. Consequently, the intensity of the γ 2021.8-keV and γ 2052.9-keV peaks in Spectrum I is expected to be 1.3 and 5.1 events, respectively. According to our estimations, the average background in the region 2000–2060 keV of Spectrum I is 10 events/keV or 0.18 events/(keV · kg · y), which agrees with background measurements in [5, 10, 19, 21]. Considering the resolving power of the detectors (FWHM \cong 3.5 keV), the expected intensities of the 2021.8-keV and 2052.9-keV peaks should exceed the average background by approximately 4 and 15%, respectively. This is why the statement of C. E. Aalseth et al. [7] and Yu. G. Zdesenko et al. [9] that weak ^{214}Bi peaks could not be observed in [3, 4] should be thought of as somewhat premature, at least for the γ 2052.9-keV peak. Estimates of expected intensities of peaks from the ^{214}Bi decay in Table 4 are not in conflict with the fact that the peaks at 2021.8 and 2052.9 keV and the peak at 2039 keV reported in [3–5] are really observed in the Heidelberg–Moscow experiment.

Row 5 of Table 4 presents intensities of weak ^{214}Bi peaks calculated in [5, 10] with allowance for summation of pulses from the cascade γ transitions (simulation of the γ spectrum with the fitted location of ^{214}Bi nuclei in the vicinity of the detectors). As expected, the intensities of the γ 2021.8-keV and γ 2052.9-keV peaks did not change in comparison with the calculations (rows 3 and 4), while intensities of the γ 2010.7-keV and γ 2016.7-keV peaks appreciably increased. In [5, 10] they arrive at the conclusion that the calculated expected intensities of the peaks agree with the experimental values within double the experimental error. It is noteworthy that the calculated intensities of the γ 2021.8-keV and γ 2052.9-keV peaks are a few times smaller than the experimental ones, while the calculated and experimental intensities of the γ 2010.7-keV and γ 2016.7-keV peaks are close in value.

We have considered possibilities of the 2039-keV peak being formed in the spectrum as a result of detecting γ rays from the decay of radioactive nuclides which may be present in the setup as natural impurity or may be produced in the structural materials as a result of interaction with background neutrons or muons. In our consideration we used the entire list of γ rays emitted by radioactive nuclides [22] and the TI [6]. We did not find any possibility for that. To illustrate, let us consider two cases of radioactive nuclear decay giving rise to γ rays of energy close to 2039.0 keV.

Among all isotopes identified in the background spectrum only ^{234m}Pa ($T_{1/2} = 1.17$ min) emits γ rays of energy close to 2039.0 keV ($E_\gamma = 2041.2$ keV, $I_\gamma = 1.1 \cdot 10^{-4}\%$ of decays) [23]. The background spectrum of the Heidelberg–Moscow experiment [19] shows 1000-keV γ rays ascribed to the ^{234m}Pa decay. The intensity of this γ transition, the strongest in the ^{234m}Pa decay, is 0.84% of decays [6]. The area of the γ 1000-keV peak in Spectrum I is 90(50) events. Thus, the area of the γ 2041.2 peak in Spectrum I is estimated at 0.020 events. Clearly, these γ rays cannot make a noticeable contribution to the 2039-keV peak because, according to Table 4, its intensity is 12.1(83) events.

2037.2-keV γ rays arise from the β^- decay of ^{77}Ge ($T_{1/2} = 11.3$ h). This nuclide may be produced in the reaction $^{76}\text{Ge}(n, \gamma)^{77}\text{Ge}$. Yet, the ^{77}Ge decay gives rise to 1999.6-keV γ rays with an intensity ten times as high as that of 2037.2-keV γ rays. However, 1999.6-keV γ rays were not observed in [3–5]. Note that γ rays resulting from the β^- decay of nuclides occurring in the material of the detectors do not form peaks because summation of pulses from β particles with pulses from γ rays smear out any lines.

CONCLUSION

Thus, our analysis of the spectra from the Heidelberg–Moscow experiment kindly provided by Prof. Klapdor-Kleingrothaus allows the following conclusions.

Firstly, the Heidelberg–Moscow experiment shows the best suppression of the background among low-background experiments. There is no experimental evidence for a contribution to the background spectrum from external sources (rocks in the background laboratory). The γ rays observed in the background spectrum in the region up to 3200 keV arise from the decay of trace amounts of anthropogenic or cosmogenic nuclides contaminating the setup between the detectors and the main shielding.

Secondly, contrary to previous opinions, γ rays of ^{226}Ra and daughter nuclides are shown to arise in the radium-226 rather than uranium-238 equilibrium chain.

Thirdly, the expected intensities of weak ^{214}Bi γ lines in the spectral region of 2000–2060 keV determined by a direct comparison to strong Bi lines in the spectrum do not contradict the fact that these lines, and the 2039.0-keV line caused by detection of two β particles from the $0\nu 2\beta$ decay of ^{76}Ge [3], are really observed in this experiment. The statistics gained after the year 2000 and the pulse-shape analysis of events in the 2039.0-keV peak confirm this conclusion (see, for example, [11–18]).

The results obtained may help both to confirm observation of the 2039-keV line from the $0\nu 2\beta$ decay of ^{76}Ge in the Heidelberg–Moscow experiment and to design new low-background experiments.

Acknowledgements. The authors are grateful to Prof. H. V. Klapdor-Kleingrothaus for providing background spectra of the Heidelberg–Moscow experiment and for helpful discussions. The investigation was supported by the Russian Foundation for Basic Research (projects 04-02-17144 and 02-02-04009).

REFERENCES

1. Schechter J., Valle J. W. F. // Phys. Rev. D. 1982. V. 25. P. 2951.
2. Klapdor-Kleingrothaus H. V. et al. // Eur. Phys. J. A. 2001. V. 12. P. 147.
3. Klapdor-Kleingrothaus H. V. et al. // Mod. Phys. Lett. A. 2001. V. 16. P. 2409.
4. Klapdor-Kleingrothaus H. V., Dietz A., Krivosheina I. V. // Part. Nucl., Lett. 2002. No. 1[110]. P. 57.
5. Klapdor-Kleingrothaus H. V., Dietz A., Krivosheina I. V. // Found. Phys. 2002. V. 32. P. 1181; Erratum // Found. Phys. 2003. V. 33. P. 679.
6. Firestone R. B., Shirley V. S. Table of Isotopes. 8th ed. J. Wiley and Sons, 1998.
7. Aalseth C. E. et al. // Mod. Phys. Lett. A. 2002. V. 17. P. 1475.
8. Feruglio F., Strumia A., Vissani F. // Nucl. Phys. B. 2002. V. 637. P. 345; Addendum // Nucl. Phys. B. 2003. V. 659. P. 359.
9. Zdesenko Yu. G., Danevich F. A., Tretyak V. I. // Phys. Lett. B. 2002. V. 546. P. 206.
10. Klapdor-Kleingrothaus H. V. hep-ph/0205228.

11. *Klapdor-Kleingrothaus H. V.* hep-ph/0302237.
12. *Klapdor-Kleingrothaus H. V.* // Intern. J. Mod. Phys. A. 2003. V. 18. P. 4113.
13. *Klapdor-Kleingrothaus H. V. et al.* // Nucl. Instr. Meth. A. 2003. V. 510. P. 281.
14. *Klapdor-Kleingrothaus H. V. et al.* // Ibid. V. 511. P. 335.
15. *Klapdor-Kleingrothaus H. V. et al.* // Phys. Lett. B. 2004. V. 578. P. 54.
16. *Klapdor-Kleingrothaus H. V. et al.* // Nucl. Instr. Meth. A. 2004. V. 522. P. 371.
17. *Klapdor-Kleingrothaus H. V. et al.* hep-ph/0404062.
18. *Klapdor-Kleingrothaus H. V. et al.* // Phys. Lett. B. 2004. V. 586. P. 198.
19. *Dörr C., Klapdor-Kleingrothaus H. V.* // Nucl. Instr. Meth. A. 2003. V. 513. P. 596.
20. *Gunther M. et al.* // Phys. Rev. D. 1997. V. 55. P. 54.
21. *Bakalyarov A. M. et al.* // Part. Nucl., Lett. 2005. V. 2, No. 2(125). P. 21.
22. *Reus U., Westmeier W.* A compilation of gamma-rays originating from radioactive decay. Inst. Nucl. Chemistry; University of Marburg, 1992.
23. *Brudanin V. B. et al.* // Part. Nucl., Lett. 2004. V. 1, No. 5(122). P. 84.

Received on May 23, 2005.